BJR

Received: 12 December 2013 | Revised: 26 February 2014 | Accepted: 5 March 2014

doi: 10.1259/bjr.20130813

Cite this article as:
Riches SF, Payne GS, deSouza NM, Dearnaley D, Morgan VA, Morgan SC, et al. Effect on therapeutic ratio of planning a boosted radiotherapy dose to the dominant intraprostatic tumour lesion within the prostate based on multifunctional MR parameters. Br J Radiol 2014;87:20130813.

FULL PAPER

Effect on therapeutic ratio of planning a boosted radiotherapy dose to the dominant intraprostatic tumour lesion within the prostate based on multifunctional MR parameters

[1]S F RICHES, PhD, [1]G S PAYNE, DPhil, [1]N M DESOUZA, MD, [2]D DEARNALEY, MD, [1]V A MORGAN, MSc, [3]S C MORGAN, MD and [4,5]M PARTRIDGE, PhD

[1]Cancer Research UK and EPSRC Cancer Imaging Centre, Royal Marsden NHS Foundation Trust and Institute of Cancer Research, Sutton, UK
[2]Academic Radiotherapy, Royal Marsden NHS Foundation Trust and Institute of Cancer Research, Sutton, UK
[3]Division of Radiation Oncology, The Ottawa Hospital Cancer Centre and the University of Ottawa, Ottawa, ON, Canada
[4]Section of Radiotherapy and Imaging, The Institute of Cancer Research, Sutton, UK
[5]The Gray Institute for Radiation Oncology and Biology, University of Oxford, Oxford, UK

Address correspondence to: Dr Sophie F. Riches
E-mail: *sophie.riches@icr.ac.uk*

Objective: To demonstrate the feasibility of an 8-Gy focal radiation boost to a dominant intraprostatic lesion (DIL), identified using multiparametric MRI (mpMRI), and to assess the potential outcome compared with a uniform 74-Gy prostate dose.
Methods: The DIL location was predicted in 23 patients using a histopathologically verified model combining diffusion-weighted imaging, dynamic contrast-enhanced imaging, T_2 maps and three-dimensional MR spectroscopic imaging. The DIL defined prior to neoadjuvant hormone downregulation was firstly registered to MRI-acquired post-hormone therapy and subsequently to CT radiotherapy scans. Intensity-modulated radiotherapy (IMRT) treatment was planned for an 8-Gy focal boost with 74-Gy dose to the remaining prostate. Areas under the dose–volume histograms (DVHs) for prostate, bladder and rectum, the tumour control probability (TCP) and normal tissue complication probabilities (NTCPs) were compared with those of the uniform 74-Gy IMRT plan.
Results: Deliverable IMRT plans were feasible for all patients with identifiable DILs (20/23). Areas under the DVHs were increased for the prostate (75.1 ± 0.6 *vs* 72.7 ± 0.3 Gy; $p < 0.001$) and decreased for the rectum (38.2 ± 2.5 *vs* 43.5 ± 2.5 Gy; $p < 0.001$) and the bladder (29.1 ± 9.0 *vs* 36.9 ± 9.3 Gy; $p < 0.001$) for the boosted plan. The prostate TCP was increased (80.1 ± 1.3 *vs* 75.3 ± 0.9 Gy; $p < 0.001$) and rectal NTCP lowered (3.84 ± 3.65 *vs* 9.70 ± 5.68 Gy; $p = 0.04$) in the boosted plan. The bladder NTCP was negligible for both plans.
Conclusion: Delivery of a focal boost to an mpMRI-defined DIL is feasible, and significant increases in TCP and therapeutic ratio were found.
Advances in knowledge: The delivery of a focal boost to an mpMRI-defined DIL demonstrates statistically significant increases in TCP and therapeutic ratio.

Phase III trials using conformal external beam radiotherapy have shown that a dose escalation improves biochemical progression-free survival in patients with prostate cancer;[1–5] however, increases in late rectal and urinary morbidity are associated with the dose distributions used to achieve these gains.

With the advent of intensity-modulated radiotherapy (IMRT), complex three-dimensional (3D) dose distributions can be delivered to areas of disease whilst reducing the dose to the surrounding tissues and also potentially boosting the dose to encompassed small volumes such as the dominant intraprostatic lesions (DILs). This is potentially advantageous, as local recurrence has been shown to originate within the initial tumour volume.[6]

This approach requires reliable and reproducible imaging to identify the DIL. Conventional MR using high spatial resolution T_2 weighted (T2W) contrast has insufficient sensitivity and specificity for defining the tumour within the prostate gland, especially if the lesions are <1 cm in diameter.[7] A combination of MRI methods whose contrast is determined by tissue physiology and biochemistry rather than anatomy offers improved sensitivity and specificity for

delineation of prostate cancers. Functional methods include diffusion-weighted imaging, MR spectroscopic imaging (MRSI) and dynamic contrast-enhanced MRI (DCE-MRI) and together present a multiparametric MRI (mpMRI) data set. We have previously validated a multiparametric model to identify prostate cancer and the location of DILs with histology from prostatectomy specimens.[8]

mpMRI data are reliable only if acquired before androgen deprivation (hormone) therapy, as there is profound functional signal degradation after hormone therapy.[9–11] Our standard institutional practice for intermediate- and high-risk localized prostate cancer uses hormone therapy for 3–6 months prior to external beam radiotherapy,[12–14] so modelling a radiation boost to mpMRI-defined tumour nodules requires acquisition of functional data before hormone therapy to be registered with anatomical images obtained post hormone treatment and immediately prior to radiotherapy[15] in order to translate the tumour location to radiotherapy planning CT images. The aim of this planning study therefore was to demonstrate the use of a mpMRI-defined DIL to create a radiotherapy boost volume. IMRT treatment plans were optimized to deliver either a uniform 74 Gy to the whole prostate or to add an 8-Gy simultaneous integrated boost to the DIL, and the potential clinical outcomes compared using dose–volume histograms (DVHs) and radiobiological models for tumour control probability (TCP) and normal tissue complication probabilities (NTCPs).

METHODS AND MATERIALS

This study was approved by the Institutional Review Board and local ethics committee. 30 patients with organ-confined disease scheduled for external beam radiotherapy were recruited. Seven patients were withdrawn after the first MR study, as the imaging observations resulted in an alteration in their management.

Pre-hormone treatment imaging

Patients were scanned supine on a flat Siemens 1.5T MAGNETOM® (Avanto; Siemens Medical Solutions, Erlangen, Germany) MRI couch feet first with an endorectal receiver (ER) coil inserted and inflated with 60 ml of air. Knee wedges and foot stocks were used to reproduce the radiotherapy treatment position. An external body radiofrequency (RF) receive array coil was centred anteriorly over the prostate. A 20-mg intramuscular injection of butylscopolamine bromide (Buscopan®; Boehringer Ingelheim, Germany) was given just prior to the acquisition to reduce peristalsis. Axial T2W images [repetition time (TR)/echo time (TE) = 4260/108 ms; field of view (FOV) = 150 mm^2; 512 × 512 matrix; 2 averages, 20 × 3 mm contiguous slices] and single-shot echoplanar imaging diffusion-weighted images (TR/TE = 4500/66 ms; FOV = 192 mm^2; 128 × 128 matrix; 4 averages; 20 × 3 mm contiguous slices with b = 0, 100, 300, 500 and 800 s mm^{-2}) were acquired. A multi-echo sequence (TR = 2200 ms; TE = 30, 60, 90, 120 ms; FOV = 192 mm^2; 128 × 128 matrix; two averages, 20 × 3 mm contiguous slices with 150-mm lateral saturation bands) was acquired in the same position. 3D MRSI was acquired (TR/TE = 700/120 ms; FOV 84 × 60 × 96 mm; 14 × 10 × 10 matrix interpolated to 16 × 16 × 16 with dual lipid and water suppression; 5 signal averages; and a central offset frequency of 1.8 parts per million) with 8 saturation slabs placed around the prostate to reduce lipid contamination. In the same location as the axial T2W images, 3D gradient-echo DCE-MRI images were acquired with a generalized autocalibrating partially parallel acquistion (GRAPPA) factor of 2 comprising a proton density image (TR/TE 3.0/1.2 ms; FOV = 350 mm^2; 128 × 128 matrix; 14 × 6 mm contiguous slices; 8 averages; flip angle 5°; 3.3 s) followed by a dynamic series (identical parameters except flip angle = 16°; 1 average; 77 timepoints; 4 min 14 s). A dose of 0.2 mmol kg^{-1} of body weight of Magnevist® (Bayer, Whippany, NJ) contrast agent at a flow rate of 3 ml s^{-1} followed by a 20-ml saline flush was injected via a power injector at the start of the third timepoint. All axial images and the MRSI grid were truly transverse, with no angles relative to the scanner axis. After acquisition of the functional MR data, the ER coil was removed without moving the patient and a set of true axial T2W images were acquired with the external RF receive coils only.

Neoadjuvant hormone therapy

Immediately following the initial MR scan, patients began a 12-week course of hormone therapy. After approximately 8 weeks, gold seed fiducial markers were inserted into the prostate gland under transrectal ultrasound guidance; these markers are visible on both CT and MR imaging and allow registration of the image sets. After 12 weeks, radiotherapy planning CT scans were obtained following a bladder filling protocol, which entailed bladder emptying followed by an oral fluid load of 350 ml of water in 1 h.

Post-hormone treatment imaging

Post-hormone treatment MR images were obtained 24 h after the planning CT, and patients followed an identical bladder filling and positioning protocols. Anterior skin tattoos on the patients' symphysis pubis were aligned with the MR scanner sagittal laser, and the transverse hip angle minimized by alignment of the lateral skin tattoos with the scanner lateral lasers. True axial T2W and dual-echo images (TE, 2.38/5.32 ms) were acquired with external array receiver coils.

Data processing

Monoexponential T_2 and apparent diffusion coefficent (ADC) maps were calculated using an inhouse IDL® v. 7.1 (Exelis Visual Information Solutions, Boulder, CO) processing programme. The first and last three slices of the DCE-MRI acquisition were not processed owing to signal instabilities. Gross movement was corrected on a frame-by-frame basis. A pharmacokinetic extended kety (cosine) model was used to calculate the transfer constant for blood plasma to extravascular extracellular space (EES), K^{trans}, the transfer constant from the EES back to the blood plasma (k_{ep}), the initial area under the gadolinium concentration curve, initial area under the gadolinium curve (IAUGC) and the total EES volume (V_e). The input parameters were derived from an arterial input function (AIF) model[16] fitted to the population averaged input function[17] using MFI Workbench software.[18] The metabolite MRSI for each slice was processed using LCModel v. 6.1 (Stephen Provencher Inc, Oakville, ON)[19] with a prostate basis file containing choline, creatine and citrate, giving a peak area ratio of choline + creatine to citrate and Cramér–Rao bound estimates of the errors of the

fit. An inhouse IDL programme aligned the spectroscopy data with the T_2 images using slice position and rotation in digital imaging and communications in medicine (DICOM) header information to find the coincident position of the two data sets.

Multiparametric classification of prostate tissue type

In order to classify the prostate tissues as either tumour or non-tumour, a model previously validated against histopathology from radical prostatectomy samples was used[8] to identify the DILs. All data were re-sampled to the size of the MRSI voxels. A discriminant function for the tissue type represented by each voxel was calculated and compared with the validated tumour threshold to determine whether or not it was tumorous. Dominant lesions were identified manually from tumour maps and if no obvious lesion was dominant then all tumour regions greater in size than four adjacent MRSI voxels were included.

Registration of dominant lesions to non-endorectal, post-hormone and CT images

In order to localize the dominant lesion on the radiotherapy planning CT images, registration was performed in three stages. Initially, the ER images acquired prior to hormone treatment were registered with the pre-hormone therapy non-ER images to correct the distortion of the gland due to the endorectal coil. This was done by aligning the centre of whole prostate and central gland outlines on the images to correct the scaling and rigid-body shift of the prostate, followed by non-rigid registration of anatomical features in the prostate and the peripheral zone and central gland outlines. Secondly, the shrinkage of prostate and tumour during 12 weeks of hormone therapy was accounted for by registering outlines drawn round the whole prostate and central gland on the pre- and post-hormone therapy non-ER T2W images using a bilinear scaling algorithm to map the position of the pre-hormone DIL on the post-hormone images, accounting for the difference in shrinkage of the peripheral zone and central gland tissues.[15] Finally, the post-hormone therapy non-ER images were registered with the planning CT images by rigid-body registration of the fiducial markers visible in the dual-echo and CT images.

Radiotherapy planning of a boosted dose to the dominant lesion

The radiotherapy planning was performed using Pinnacle radiotherapy planning software v. 9.4 (Philips Medical Systems, Best, Netherlands). The gross tumour volume (GTV) was defined as the mpMRI tumour. A focal boost planning target volume (PTV) was defined as PTV_82 Gy (GTV + 2-mm isotropic expansion within the gland), and three PTVs were defined using guidelines from the national CHHiP trial (ISRCTN97182923[14]): PTV_74 Gy (prostate + 3-mm margin in all directions except 0 mm posteriorly), PTV_71 Gy (PTV_74 Gy + 3 mm) and PTV_60 Gy (prostate + seminal vesicles + 6-mm isotropic expansion). The reduced margin in the boost volume compared with the prostate is a pragmatic compromise between coverage and organ at risk sparing; very large risks of overdosing the organs at risk whilst underdosing due to motion is preferable as the surrounding tissue will receive 74 Gy anyway.

A class solution with five 6-MV beams was used with posterior, left-posterior-oblique, right-posterior-oblique, left-anterior-oblique and right-anterior-oblique fields. A 0.25-cm dose calculation grid was applied and 2.22 Gy per fraction to 100% of PTV_82 Gy was prescribed for 37 fractions. IMRT optimization using an adaptive collapsed cone convolution algorithm was performed with 50 iterations attempting to achieve the objectives shown in Table 1.

For the standard plan, the three PTVs (PTV_74 Gy, PTV_71 Gy and PTV_60 Gy) were defined using the same margins as the boosted plan, and the same objectives (with the omission of PTV_82 Gy) were used. Both plans were optimized until they met mandatory clinical constraints for rectal and bladder dose without compromising the target coverage;[20] optimal constraints were met where possible. Doses received by 98%, 50% and 2% of each PTV were noted. For the rectum, the percentage volume receiving 30, 40, 50, 60, 65, 70 and 74 Gy and the dose received by 2% of the rectum were noted. For the bladder, the percentage volume receiving 50, 60, 74 and 80 Gy was noted and for patients with the urethra outlined, the doses received by 50% and 2% were calculated. DVHs for PTV_74 Gy, the bladder and rectum were calculated for each patient and a paired *t*-test was used to determine differences in the areas from the rival plans at the 5% significance level.

Radiobiological modelling

The TCP was calculated for each patient using the logistic model of King and Kapp[21] (biochemical control at 5 years, radical radiotherapy series):

$$\mathrm{TCP}=\frac{e^{\left(\frac{d-\mathrm{TCD}_{50}}{k}\right)}}{1+e^{\left(\frac{d-\mathrm{TCD}_{50}}{k}\right)}}$$

where d is total dose, TCD_{50} is the dose required to achieve 50% biochemical tumour = 65.9 Gy and k is a fitting parameter related to the slope at the TCD_{50} point = 9.61.

For the bladder and rectum, the NTCP was calculated as the integral over dose intervals t,

$$\mathrm{NTCP}=\frac{1}{2\pi}\int_{-\infty}^{u} e^{\frac{t^2}{2}}\cdot dt$$

where

$$u=\frac{D-\mathrm{TD50}(V)}{m\times\mathrm{TD50}(V)},\ \text{and}\ \mathrm{TD50}(V)=\frac{\mathrm{TD50}(1)}{V^n}$$

where TD50(1) is the tolerance dose to an organ for 50% of patients to experience a defined complication, TD50(V) is the tolerance dose for a partial volume (V), m accounts for the standard deviation (SD) of V and n accounts for the degree of parallel structure in the organ.

For the rectum, rectal NTCP ($\mathrm{NTCP}_{\mathrm{rectum}}$) was calculated for Grade 2 rectal bleeding, and values of TD50(1), m and n were taken as 68.5 Gy, 0.15 and 0.13, respectively.[22] For the bladder, bladder NTCP ($\mathrm{NTCP}_{\mathrm{bladder}}$) was calculated for Grade 1 genitourinary toxicity at 2 years, and values of TD50(1), m and n

Table 1. Objectives for different structures optimized in the intensity-modulated radiotherapy treatment boosted radiotherapy plan

Structure	Objective	Dose (Gy)	Volume (%)	Weight (%)
PTV_82 Gy	Min DVH	82.00	50	75
	Min dose	77.00		70
PTV_74 Gy	Min DVH	74.00	50	100
	Min dose	70.30		70
PTV_71 Gy	Min DVH	71.00	52	100
	Min dose	67.50		80
PTV_60 Gy	Max DVH	61.00	50	1
	Min DVH	60.00	50	100
	Min dose	57.00		100
Bladder	Max DVH	60.00	15	20
	Max DVH	50.00	40	20
	Max dose	74.00		50
Bladder-PTV_60 Gy	Max dose	67.34		50
Rectum	Max DVH	30.00	65	20
	Max DVH	60.00	25	15
	Max DVH	74.00	2	30
	Max DVH	50.00	45	15
	Max dose	77.00		50
Bowel	Max dose	50.00		5
Left femoral head	Max dose	50.00		1
Right femoral head	Max dose	50.00		1

DVH, dose–volume histogram; Max, maximum; Min, minimum; PTV, planning target volume.

were taken as 77.6 Gy, 0.022 and 0.00995, respectively.[23] The rival plans were compared using a paired *t*-test with 5% significance level to test for differences in the mean calculated TCP, $NTCP_{bladder}$ and $NTCP_{rectum}$.

RESULTS

The ages of the patients were [median (range)] 70 (58–80) years. Stages were T1b ($n = 1$), T1c ($n = 12$), T2a ($n = 8$), T2c ($n = 1$) and T3a ($n = 1$). Gleason grades were $3 + 3$ ($n = 8$), $3 + 4$ ($n = 11$) and $4 + 3$ ($n = 4$), and prostate-specific antigen (PSA) was mean ± SD, (range) 14 ± 10 (5–46) ng ml^{-1}.

A full set of mpMRI data was acquired for all patients and parametric maps were generated at MRSI voxel resolution (Figure 1). 15 patients had 1 dominant lesion and 5 had 2 lesions. Eight lesions were in the peripheral zone, eight were in the central gland and ten covered both tissues. Three patients had no identifiable dominant lesion; two had tumour regions identified throughout the prostate and one had very small amounts of tumour identified. 22 patients had 3 gold seed fiducial markers inserted and 1 patient had 4 seeds inserted within the prostate gland. The average time [mean ± SD (range)] between the insertion of the gold seeds and second MR studies was 32 ± 5 (25–39) days. Gold seeds were visible on the dual-echo T_1 weighted images in post-hormone scans for all patients. The scaling algorithm was applied to the non-ER pre-hormone treatment images and resulted in post-hormone DIL targets in all patients who had identified dominant lesions. The average time between the first and second MR studies was 85 ± 7 (range, 68–96) days. The average residual distance between the gold seeds after the rigid-body alignment with CT was 0.09 ± 0.05 (range, 0.007–0.19) cm. The average (mean ± SD) rotations of the MRI block were −1.87 ± 3.80°, −0.01 ± 3.91° and −0.31 ± 2.76° in the left–right, anterior–posterior and foot–head planes, respectively. The average [mean ± SD (range)] volume of the mpMRI-defined GTV on the CT planning images was 3.91 ± 3.04 (0.8–10.4) cm^3.

Radiotherapy planning

Lateral hotspots were observed in 11/20 patients; these were removed by the addition of a planning objective in the region of the hotspot in all cases. It was possible to plan a focal boost of 8 Gy to the mpMRI-defined GTV plus an intraprostatic margin of 2 mm in all patients whilst meeting the mandatory constraints. Target coverage for all the DILs was good; compared with the standard plan, the doses received by 98%, 50% and 2% of the PTV_74 Gy (excluding the PTV_82 Gy region) were greater, as expected. The doses achieved by 98%, 50% and 2% of PTV_74 Gy

Figure 1. Tumour (outline) identified by functional MR on (top row, from left) T_2 weighted image, ADC map, T_2 map (bottom row, from left), choline + creatine/citrate, K^{trans} and initial area under the gadolinium curve (IAUGC).

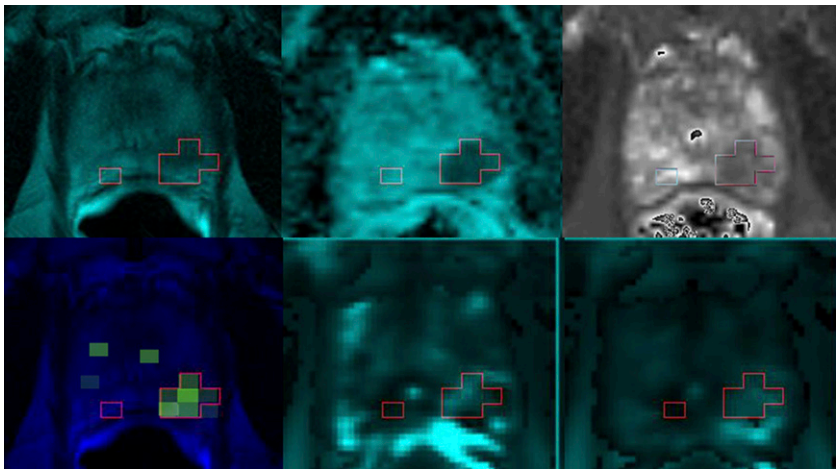

and PTV_82 Gy of the boosted radiotherapy plan and the PTV_74 Gy for the standard plan are given in Table 2.

Tissue constraints

Doses received by the rectum and bladder, compared with mandatory and optimal constraints, are shown in Figure 2. All constraints for rectum and mandatory constraints for bladder were met for all 20 patients; the optimal constraints for bladder were met for 15/20 patients. The urethra was outlined in six patients where it was visible on the MR images; for these patients the dose [mean ± SD (range)] received by 50% and 2% of the structure was 78.3 ± 2.8 (75.4–81.8) and 80.8 ± 2.0 (78.1–82.4) Gy, respectively.

Dose–volume histograms

Areas under the cumulative DVHs (Figure 3) for the PTV_74 Gy, bladder and rectum for the standard and boosted radiotherapy plans are given in Table 3. Paired *t*-tests showed a significant increase in the area under the DVH of the PTV_74 Gy (excluding the PTV_82 Gy; $p < 0.001$) and significant decreases in the areas under the curve for the rectum and bladder (both $p < 0.001$) for the boosted plan.

Radiobiological modelling

The average TCP was significantly greater for the boosted plan than that for the standard plan (80.1 ± 1.3% *vs* 75.3 ± 0.9%; $p < 0.001$). The average $NTCP_{rectum}$ was significantly lower for the boosted plan (3.84 ± 3.65% *vs* 9.70 ± 5.68%; $p = 0.04$). Calculated values for $NTCP_{bladder}$ were vanishingly small for both plans.

DISCUSSION

This study showed that clinically acceptable IMRT plans could be produced by boosting dose to mpMRI-defined DILs. Radiobiological modelling suggested significant improvements in TCP and NTCP compared with standard plans. The King logistic model fit for 5-year biochemical control from a number of radical radiotherapy trials[20] was used to estimate TCP. Androgen suppression and differences in clinical stage mix might affect the absolute radiobiological model predictions, although the use of a single model to score two rival plans for each patient should allow a reasonable relative comparison. It should also be noted that the use of single model parameters for the entire PTV might not be ideal: if a separate dose–response model were known for the DIL, this may improve predictions; however, currently no reliable data are available on this.

Calculation of the TCP for the whole prostate PTV showed a significantly greater TCP for the boosted plan than for the standard plan. The doses to the bladder were such that the NTCP in both plans were negligible using the standard Lyman–Kutcher–Burman model chosen. It was expected that the boosted plan would result in the same or higher doses to the rectum owing to the increased doses prescribed to the tumour;

Table 2. Average [mean ± standard deviation (range)] doses received by 98%, 50% and 2% of the planning target volume (PTV) in the standard and boosted radiotherapy plans

Volume	98% dose (Gy)	50% dose (Gy)	2% dose (Gy)
Standard clinical plan			
PTV_74 Gy	70.8 ± 0.5 (70.0–71.3)	73.0 ± 0.41 (72.1–73.6)	74.8 ± 0.47 (74.5–75.5)
Boosted plan			
PTV_74 Gy	71.3 ± 0.5 (70.6–72.2)	76.3 ± 0.7 (75.1–77.6)	81.9 ± 0.6 (81.0–83.4)
PTV_82 Gy	80.2 ± 0.7 (78.9–81.2)	82.0 ± 0.2 (81.6–82.4)	83.0 ± 0.6 (82.4–84.8)

Figure 2. Average (mean ± standard deviation) percentage volumes of rectum (left) and bladder (right) receiving doses for the standard and boosted dose plans (bar graphs) compared with normal tissue mandatory (open circles) and optimal constraints (filled circles) used in clinical practice to decide if a plan is acceptable.

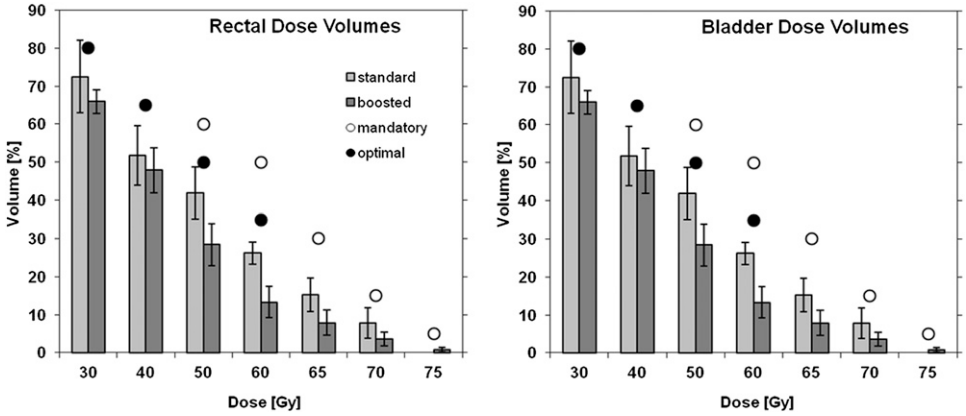

however, the boosted plans gave a significantly lower rectal NTCP. As there was no difference in the definition of the normal structures, margins on the comparable PTVs or normal tissue constraints were used to optimize the two rival plans. The only difference was relaxation of the implicit constraint within the optimizer to produce a uniform PTV dose distribution. The additional degree of freedom allowing a "hot spot" with the PTV (the boost volume) seems to have enabled the optimizer to better spare the rectal wall in these cases. Although beneficial in the cases shown here, this result should be interpreted with caution and might not generalize to other delivery class solutions or optimization algorithms.

Previous attempts to plan a boosted IMRT dose of 90 Gy to a target defined by T2W and MRSI data have indicated an increased TCP and decreased NTCP compared with uniform 3D conformal radiotherapy.[24] A similar methodological approach by De Meerleer et al[25] planning a boosted dose of 80 Gy to the target and 70 Gy to the rest of the prostate showed a small increase in TCP for the boosted dose and no difference in the rectal NTCP; although our study showed lower TCP values than theirs (80.1% *vs* 92.1%—potentially due to the use of a different TCP model) we report a lower rectal NTCP in the boosted plan. Delivery of boosted radiotherapy doses based on mpMRI currently remains anecdotal, although there is a large-scale randomized trial underway (NCT01168479): Singh et al[26] successfully boosted a dose to 84.5 Gy for three patients using radiologist-defined tumour based on T2W, MRSI and DCE-MRI images and reported rectal doses of <7 Gy compared with 3.6 Gy in our study. They achieved maximum urethral doses in the 78.4–79.2 Gy range, which is similar to the urethral values reported in the six patients we evaluated in this study. Another study of five patients[27] used a balloon coil with identical proportions to the MR endorectal coil for CT planning and treatment, eliminating the requirement for correction of the prostatic compression due to the coil. In that study, patients did not receive neoadjuvant hormone therapy, negating the need to correct for the shrinkage of the gland with this treatment prior to radiotherapy. They reported $NTCP_{rectum}$ to be reduced in four out of five patients, but they did not find a significant increase in TCP (78 Gy: 86% ± 2%, 70 + 90 Gy boost: 86% ± 2%); this is because they reduced the whole prostate dose in the boosted plan compared with the uniform dose plan.

Miralbell et al[28] gave a hypofractionated boosted dose of 10, 12 or 14 Gy to an MR-defined lesion after 64 Gy to the rest of the prostate using a rectal balloon for radiotherapy treatment to improve MR positioning, and reported 5-year biochemical disease-free and disease-specific survival were 98% ± 1.9% and 100%, respectively. However, 32/50 patients received 3 months of androgen therapy between the MR image acquisition and the radiotherapy planning study. Androgen therapy has been shown to cause considerable shrinkage of the prostate, which is greater in the peripheral zone than that in the central gland. As such,

Figure 3. Cumulative dose–volume histograms for the PTV_74 Gy for the standard clinical and boosted (solid: average, dotted: 95% confidence limits) intensity-modulated radiotherapy treatment plan for PTV_74 Gy (left), rectum (centre) and bladder (right). PTV, planning target volume.

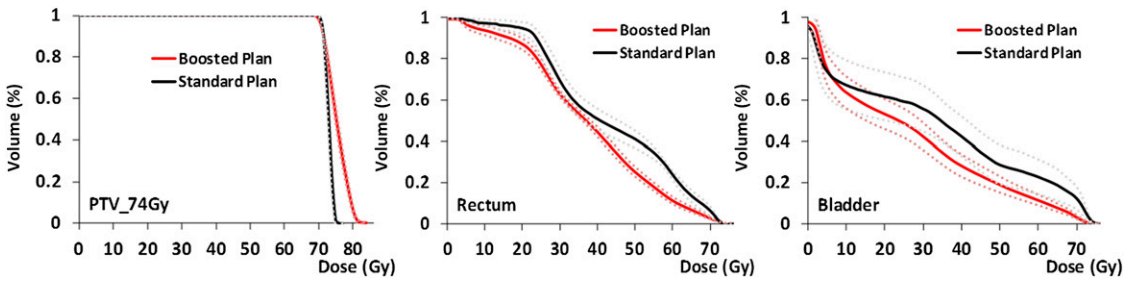

Table 3. Areas under the cumulative dose–volume histograms for the PTV_74 Gy, rectum and bladder for the standard and boosted plans

Structure	Standard clinical plan	Boosted plan
PTV_74 Gy	72.7 ± 0.4 (72.2–73.1)	75.10 ± 0.6 (74.2–76.4)
Rectum	43.5 ± 2.5 (40.0–46.8)	38.2 ± 2.5 (34.0–40.9)
Bladder	36.9 ± 9.3 (27.8–56.1)	29.2 ± 9.0 (17.8–46.4)

PTV, planning target volume.

registration of the T2W MR images to the radiotherapy planning images might have resulted in inaccurate placement of the dominant lesion within the gland. Our study uses a bilinear algorithm to account for this tissue shrinkage to allow a more accurate positioning of the DIL in the radiotherapy plan.

Fonteyne et al[29] defined a DIL using T2W MR signal with ($n = 52$) or without ($n = 66$) confirmation of tumour from MRSI information and treated the dominant lesion to 81 and 82 Gy, respectively, and reported that no statistically significant increase was found in Grade 2–3 acute gastrointestinal or genitourinary toxicity. However, little information is reported on how the spectroscopic information generated using an endorectal coil was registered to the T2W MR images acquired with an external coil.

Identification of the mpMRI-defined DIL was possible only for voxels where all MR parameters were defined. The resampling of the T_2, ADC and DCE-MRI maps to the MRSI voxel resolution meant that the limiting parameter was MRSI; voxels missing parameters were assumed to be non-tumour, so tumour regions might have been missed or reduced in size. Isolated tumour voxels might either have been incorrectly classified or be regions of tumour just large enough to be detected by the algorithm; in either case a focal boost is not a suitable treatment.

CONCLUSIONS

Delivery of a focal boost to DILs identified on mpMRI is possible whilst meeting current clinical mandatory constraints for normal tissues. Location of the DIL requires alignment with anatomical images acquired in a position replicating the radiotherapy treatment planning CT, scaling to account for the non-uniform shrinkage of the prostate during 12 weeks of neoadjuvant androgen deprivation hormone treatment and registration of MR and CT data using internally placed fiducial markers. Radiobiological modelling suggests that adoption of such a technique might improve the therapeutic ratio, increasing tumour control without compromising rates of normal tissue complication. We are assessing this approach in an ongoing clinical trial DELINEATE (ISRCTN04483921).

FUNDING

We acknowledge the support received for the CRUK and EPSRC Cancer Imaging Centre in association with MRC and Department of Health C1060/A10334, RM/ICR NIHR Biomedical Research Centre and the Clinical Research Facility in Imaging. Sophie Riches was funded by a Personal Award Scheme Researcher Developer Award from the NIHR. Scott Morgan was funded by a research fellowship from the Canadian Association of Radiation Oncology and Elekta AB.

REFERENCES

1. Pollack A, Zagars GK, Starkschall G, Antolak JA, Lee JJ, Huang E, et al. Prostate cancer radiation dose response: results of the M. D. Anderson Phase III randomized trial. *Int J Radiat Oncol Biol Phys* 2002; **53**: 1097–105.
2. Peeters ST, Heemsbergen WD, Koper PC, van Putten WL, Slot A, Dielwart MF, et al. Dose-response in radiotherapy for localized prostate cancer: results of the Dutch multicenter randomized Phase III trial comparing 68 Gy of radiotherapy with 78 Gy. *J Clin Oncol* 2006; **24**: 1990–6. doi: 10.1200/JCO.2005.05.2530
3. Dearnaley DP, Hall E, Lawrence D, Huddart RA, Eeles R, Nutting CM, et al. Phase III pilot study of dose escalation using conformal radiotherapy in prostate cancer: PSA control and side effects. *Br J Cancer* 2005; **92**: 488–98. doi: 10.1038/sj.bjc.6602301
4. Zietman AL, DeSilvio ML, Slater JD, Rossi CJ Jr, Miller DW, Adams JA, et al. Comparison of conventional-dose vs high-dose conformal radiation therapy in clinically localized adenocarcinoma of the prostate: a randomized controlled trial. *JAMA* 2005; **294**: 1233–9. doi: 10.1001/jama.294.10.1233
5. Beckendorf V, Guerif S, Le Prisé E, Cosset JM, Bougnoux A, Chauvet B, et al. 70 Gy versus 80 Gy in localized prostate cancer: 5-year results of GETUG 06 randomized trial. *Int J Radiat Oncol Biol Phys* 2011; **80**: 1056–63. doi: 10.1016/j.ijrobp.2010.03.049
6. Cellini N, Morganti AG, Mattiucci GC, Valentini V, Leone M, Luzi S, et al. Analysis of intraprostatic failures in patients treated with hormonal therapy and radiotherapy: implications for conformal therapy planning. *Int J Radiat Oncol Biol Phys* 2002; **53**: 595–9.
7. Kwek JW, Thng CH, Tan PH, Yuen JS, Khoo JB, Quek ST, et al. Phased-array magnetic resonance imaging of the prostate with correlation to radical prostatectomy specimens: local experience. *Asian J Surg* 2004; **27**: 219–24; discussion 225–6. doi: 10.1016/S1015-9584(09)60037-3
8. Riches S, Payne GS, Partridge M, Jameson C, Odgen C, Morgan V, et al. Optimal combined functional MR parameters to correctly identify tumour in the prostate. *Proc Intl Soc Mag Reson Med* 2013; **44**: 100.
9. Riches SF, Morgan V, Payne GS, Dearnaley D, deSouza N. Diffusion weighted imaging of androgen deprivation hormone therapy prostate cancer patients. *Proc Intl Soc Mag Reson Med* 2007; 793.
10. Mueller-Lisse UG, Swanson MG, Vigneron DB, Hricak H, Bessette A, Males RG, et al.

Time-dependent effects of hormone-deprivation therapy on prostate metabolism as detected by combined magnetic resonance imaging and 3D magnetic resonance spectroscopic imaging. *Magn Reson Med* 2001; **46**: 49–57.

11. Padhani AR, MacVicar AD, Gapinski CJ, Dearnaley DP, Parker GJ, Suckling J, et al. Effects of androgen deprivation on prostatic morphology and vascular permeability evaluated with mr imaging. *Radiology* 2001; **218**: 365–74. doi: 10.1148/radiology.218.2.r01ja04365
12. Denham JW, Steigler A, Lamb DS, Joseph D, Turner S, Matthews J, et al. Short-term neoadjuvant androgen deprivation and radiotherapy for locally advanced prostate cancer: 10-year data from the TROG 96.01 randomised trial. *Lancet Oncol* 2011; **12**: 451–9. doi: 10.1016/S1470-2045(11)70063-8
13. Dearnaley DP, Sydes MR, Graham JD, Aird EG, Bottomley D, Cowan RA, et al. Escalated-dose versus standard-dose conformal radiotherapy in prostate cancer: first results from the MRC RT01 randomised controlled trial. *Lancet Oncol* 2007; **8**: 475–87. doi: 10.1016/S1470-2045(07)70143-2
14. Dearnaley D, Syndikus I, Sumo G, Bidmead M, Bloomfield D, Clark C, et al. Conventional versus hypofractionated high-dose intensity-modulated radiotherapy for prostate cancer: preliminary safety results from the CHHiP randomised controlled trial. *Lancet Oncol* 2012; **13**: 43–54.
15. Riches S, Partridge M, Payne GS, Morgan VA, deSouza NM. Scaling methods for registration of pre- and post-androgen ablation MR prostate images. *Proc Intl Soc Mag Reson Med* 2009; **17**: 2908.
16. Orton MR, d'Arcy JA, Walker-Samuel S, Hawkes DJ, Atkinson D, Collins DJ, et al. Computationally efficient vascular input function models for quantitative kinetic modelling using DCE-MRI. *Phys Med Biol* 2008; **53**: 1225–39. doi: 10.1088/0031-9155/53/5/005
17. Parker GJ, Roberts C, Macdonald A, Buonaccorsi GA, Cheung S, Buckley DL, et al. Experimentally-derived functional form for a population-averaged high-temporal-resolution arterial input function for dynamic contrast-enhanced MRI. *Magn Reson Med* 2006; **56**: 993–1000. doi: 10.1002/mrm.21066
18. d'Arcy JA, Collins DJ, Padhani AR, Walker-Samuel S, Suckling J, Leach MO, et al. Magnetic resonance imaging workbench: analysis and visualization of dynamic contrast-enhanced MR imaging data. *Radiographics* 2006; **26**: 621–32. doi: 10.1148/rg.262045187
19. Provencher SW. Automatic quantitation of localized *in vivo* 1H spectra with LCModel. *NMR Biomed* 2001; **14**: 260–4.
20. Gulliford SL, Foo K, Morgan RC, Aird EG, Bidmead AM, Critchley H, et al. Dose–volume constraints to reduce rectal side effects from prostate radiotherapy: evidence from MRC RT01 Trial ISRCTN 47772397. *Int J Radiat Oncol Biol Phys* 2010; **76**: 747–54. doi: 10.1016/j.ijrobp.2009.02.025
21. King CR, Kapp DS. Radiotherapy after prostatectomy: is the evidence for dose escalation out there? *Int J Radiat Oncol Biol Phys* 2008; **71**: 346–50. doi: 10.1016/j.ijrobp.2007.10.008
22. Gulliford SL, Partridge M, Sydes MR, Webb S, Evans PM, Dearnaley DP, et al. Parameters for the Lyman Kutcher Burman (LKB) model of Normal Tissue Complication Probability (NTCP) for specific rectal complications observed in clinical practise. *Radiother Oncol* 2012; **102**: 347–51.
23. Cheung MR, Tucker SL, Dong L, de Crevoisier R, Lee AK, Frank S, et al. Investigation of bladder dose and volume factors influencing late urinary toxicity after external beam radiotherapy for prostate cancer. *Int J Radiat Oncol Biol Phys* 2007; **67**: 1059–65. doi: 10.1016/j.ijrobp.2006.10.042
24. Pickett B, Vigneault E, Kurhanewicz J, Verhey L, Roach M. Static field intensity modulation to treat a dominant intra-prostatic lesion to 90 Gy compared to seven field 3-dimensional radiotherapy. *Int J Radiat Oncol Biol Phys* 1999; **44**: 921–9.
25. De Meerleer G, Villeirs G, Bral S, Paelinck L, De Gersem W, Dekuyper P, et al. The magnetic resonance detected intraprostatic lesion in prostate cancer: planning and delivery of intensity-modulated radiotherapy. *Radiother Oncol* 2005; **75**: 325–33.
26. Singh AK, Guion P, Sears-Crouse N, Ullman K, Smith S, Albert PS, et al. Simultaneous integrated boost of biopsy proven, MRI defined dominant intra-prostatic lesions to 95 gray with IMRT: early results of a Phase I NCI study. *Radiat Oncol* 2007; **2**: 36. doi: 10.1186/1748-717X-2-36
27. van Lin EN, Fütterer JJ, Heijmink SW, van der Vight LP, Hoffmann AL, van Kollenburg P, et al. IMRT boost dose planning on dominant intraprostatic lesions: gold marker-based three-dimensional fusion of CT with dynamic contrast-enhanced and 1H-spectroscopic MRI. *Int J Radiat Oncol Biol Phys* 2006; **65**: 291–303. doi: 10.1016/j.ijrobp.2005.12.046
28. Miralbell R, Mollà M, Rouzaud M, Hidalgo A, Toscas JI, Lozano J, et al. Hypofractionated boost to the dominant tumor region with intensity modulated stereotactic radiotherapy for prostate cancer: a sequential dose escalation pilot study. *Int J Radiat Oncol Biol Phys* 2010; **78**: 50–7.
29. Fonteyne V, Villeirs G, Speleers B, De Neve W, De Wagter C, Lumen N, et al. Intensity-modulated radiotherapy as primary therapy for prostate cancer: report on acute toxicity after dose escalation with simultaneous integrated boost to intraprostatic lesion. *Int J Radiat Oncol Biol Phys* 2008; **72**: 799–807.